IMPROVING THE OPTICAL SURVEY FOR GEO SPACE OBJECTS WITH PSF MODELING AND IMAGE RESTORATION

Rongyu Sun and Shengxian Yu

Purple Mountain Observatory, Nanjing 210008, China, Email: {rysun, yusx}@pmo.ac.cn

ABSTRACT

Optical survey is an efficient technique to survey space debris, especially for the ones in MEO and GEO orbital regions. Utilizing wide field of view and relatively small aperture telescope is a popular and costless way to perform space debris surveys, however, due to the optics defects of the telescope as well as the limited aperture size, the detection ability for faint objects is affected. Here image restoration is adopted to improve the image quality and detection efficiency. To optimizing image processing, the imaging process is modeled (referred as point spread function) from raw CCD images with principal component analysis, the preliminary results are analyzed and the optimal mean point spread function is constructed, with which the image restoration is performed to improve the data quality and reduction efficiency. To test the efficiency and reliability, a survey is performed with our wide field of view ($4.4^\circ \times 4.4^\circ$) 50-cm refracting telescope. In our survey, the stare mode is adopted and the dedicated image processing pipeline for detecting GEO objects automatically is presented. Our survey lasts for 11days and it takes 4 hours each day. While the raw images are obtained, the restoration is performed with our proposed technique, then the image processing pipeline runs on both raw and restored images. The tracklets are correlated with the catalog and the improvement for object detection is investigated accordingly. The results demonstrated that with image restoration, the count of tracklets increases about 80% in average, and the count of objects detected increases more than 20% for most arcs. Due to the smear noises and unexpected impulse noises, the correlation ratio of the tracklets varies and is reduced by around 10% for most surveys. However, it should be noted that with imaging modeling and restoration, the detection ability can be improved distinctly with the present technical state of art, and it deserves wider application in optical space debris observations.

Keywords: astrometry; PSF modeling; image processing.

1. INTRODUCTION

Nowadays for large areal sky surveys which are mainly focused on detecting transient sources or fast moving near Earth objects, optical telescopes with wide field of view and appropriate aperture size play unique and significant roles[1]. The wide field of view can provide large sky areal coverage, hence the surveys for specific areas can be repeated in a shorter time span, making the observations more continuous. Meanwhile, the relatively small aperture makes the telescope relatively inexpensive and affordable from the economic point of view. However for these wide field of view and small aperture telescopes, most of them are refraction ones, the defects of the optics are distinct and it comes with a number of significant limitations that reduce sensitivity and utility of the image data. Taking the point spread function (PSF) as the response of the whole system to an ideal point source, due to the optics defects which mainly include chromatic aberrations and monochromatic aberration (e.g. spherical aberration, coma, distortion .etc), the PSF exhibits inevitable spatial and temporal variation across the field[2-3]. It should be noted that wide field of view and limited pixels of the detector yield low spatial resolution and under sampling under some circumstances, the effects of the atmospheric turbulence can be neglected according to the scale of the seeing.

Object detection with optimal precision and efficiency is of great importance for date reduction. The algorithms and techniques have been developed adequately[4-6]. However, as the defects of the optics affect the quality of images, the efficiency of source extraction is decreased accordingly. Image restoration is an efficient way to eliminate the degradation and improve data quality, it has been widely used in lots of applications, and it is proved especially effective for detecting faint sources[7-8].

In our previous work, the maximum entropy method and empirical Gaussian PSF are adopted in image restoration, the precision of astrometry for our wide field of view telescope is improved, however, as the PSF models are assumed, the differences are obvious between the given model and the true one which reveals the imaging process of the optics system, hence the promotion is limited. In further researches, the PSF model is generated from raw observation images, the principal componen-

t analysis (PCA) is utilized and the variations of the PSF are evaluated[9-11], and based on the investigations it is appropriate to take the mean PSF as the template, with which the astrometry after image restoration is improve distinctly, the efficiency of the technique is proved.

In the paper the PCA is adopted to construct the effective mean PSF for a wide field of view and small aperture telescope, then the image restoration is performed with this PSF model and the improvement of object detection is investigated. In detail, in our trial observation the space debris is surveyed, then based on the correlation with the catalogue, the object detection efficiency for raw data and data after restoration is be evaluated, the effect of our technique can be analyzed. The basic theory and method is described in Section 2, the application and the way of analysis are shown in Section 3, the results and the evaluations are presented in Section 4, in Section 5 the conclusions are drawn.

2. BASIC THEORIES AND METHOD

The principle of imaging is simple, taking $I(x, y)$ as the two-dimensional observational image obtained for a spatial linear and shift-invariant system, $O(x, y)$ is the initial ideal image, then the imaging process can be expressed as follows:

$$I(x, y) = H(x, y) \otimes O(x, y) + N(x, y) \qquad (1)$$

where $N(x, y)$ represents the noise, $\otimes$ is the convolution and (x, y) stands for the spatial coordinate of the two-dimensional image. $H(x, y)$ denotes the PSF which describes the entire imaging process, in detail it consists of the influences of the atmosphere, the optics and the sample of the detector, the exact form of $H(x, y)$ is different and complex.

In Fourier space, the equation can be transformed as follows:

$$\hat{I}(u, v) = \hat{H}(u, v) \times \hat{O}(u, v) + \hat{N}(u, v) \qquad (2)$$

where $\hat{H}(u, v)$, $\hat{I}(u, v)$, $\hat{O}(u, v)$ and $\hat{N}(u, v)$ are the transforms of the $H(u, v)$, $I(u, v)$, $O(u, v)$ and $N(u, v)$ respectively. Based upon a priori information the noise model can be assumed, then with the PSF model and the image obtained in observation, a least square method can be performed to estimate the initial image $I(x, y)$, which is supposed to be with improved image quality and better for measurement.

As mentioned above, the construction of the PSF is the key of restoration. Since the PSF describes the characteristics of the imaging system, modeling the PSF from the observational images is en efficient and reliable way. Several techniques are effective to extract the PSF from large amounts of raw data, and PCA is one of them. The aim of PCA is obtaining the optimal set of basis from large amounts of data with dimensionality reduction, then the multivariate statistics is summarized based upon the basis set, since wide field of view provides large number of background star images, it is feasible to perform PCA. The pipeline and the application in our telescope are introduced step by step as follows.

Table 1. Basic information and parameters of our refraction telescope and the CCD frame.

Parameter	Value
Diameter	500 mm
Field of view	$4.4^\circ \times 4.4^\circ$
Sensor format	2048×2048
Pixel scale	7.73 arcsec
Readout channels	2
Dynamic range	$0 \sim 65535$
CCD operating mode	Frame transfer

The first step of PSF construction is selecting appropriate samples, based on which the accurate information of the imaging can be extracted. Due to the wide field of view, a large number of background stars can be extracted from each CCD frame. A dedicated wide field of view refraction telescope is adopted, and utilizing this telescope the raw CCD images are acquired. The information of the telescope as well as the raw CCD frame acquired is shown in Table 1.

According to the detection limit and the optics defects, the images are obtained with 2 seconds exposure while the telescope is sidereal tracking. It should be noticed that the choice of exposure time is important for our reduction, if the exposure is not sufficient, the signal-to-noise ratio (SNR) of images is limited, making the images are not well-sampled and little of the sources can be extracted. While too long exposure leads to saturation and alters the shape of the PSF, especially the wings of images as the refraction optics makes the size of PSF varies significantly for different brightness stars.

In total 108 frames are acquired. At first the Tycho2 catalogue is used and the stars brighter than 12 magnitude are picked considering the detection limit of the frames. According to the influences of the wings of bright stars, to avoid the effects of the stars nearby while measuring the image intensity profile, each pair of stars is erased if the distance between them is less than 20 pixels, yielding the left star images are isolated and the PSF can be extracted more precisely. Then the theoretical positions of these left stars in the CCD frames are obtained, and around each theoretical position a sub-image with 24×24 pixels is generated, the background level of each sub-image as well as the fluctuation which is taken as the noise level is derived. Setting the threshold as three times of the noise level above the background, if more than 5 pixels are found with values greater than the threshold, the sub-image will be subtracted from the background level and kept for further reduction, otherwise the sub-image will be erased.

At last for all the left sub-images, to make the intensity distribution of the image generated with appropriate lin-

ear respond of the sensor and prevent the saturation, if the maximum of the pixel values is greater than 80% of the maximum dynamic range, the sub-image will not be processed. Otherwise, the pixel with maximum value will be taken as center and the sub-image is extracted as the sample for PSF construction.

In detail, totally 38165 stars with magnitude less than 12 are found from the catalogue in 108 frames, after the distance filtering, 14353 stars are left. With our source extraction pipeline, 13131 images are extracted, and 12610 sub-images are finally obtained after checking the maximum of pixel values.

While the large number of PSF samples is obtained, PCA is adopted to construct the high quality PSF model for image restoration. According to the basic theory, the count of samples should be much greater than the dimension of data in PCA reduction, and considering the full width at half maximum (FWHM) of the images is around 2.5 pixels, it is appropriate to take the 7×7 pixels around each sub-image center as the samples in further reduction.

Since all the PSF samples are aligned by the pixel with maximum value and the background level has been subtracted, the flux of each sample is normalized to one to eliminate the differences of PSF samples caused by the variable brightness of sources. Assuming N PSF samples with M pixels are obtained, where N refers to 12610 and M refers to 49 in our experiment. A matrix S is constructed with N rows and M columns, each row of S is a PSF sample presented in one dimension. For each column of S, the mean and deviation are obtained, and for values greater than three times of the deviation above the mean, the whole row will be considered as outliers and erased. After reduction 521 rows are erased and the final row count of S is 12089. Then the decomposition is performed as follows:

$$S = UWV^T \tag{3}$$

where U is $N \times M$ column-orthogonal matrix, W is $M \times M$ diagonal matrix, and V is $M \times M$ orthogonal matrix. Each column of V is a decomposed PSF component which is with the same size as the PSF samples, and the relative weights of these components are presented as the diagonal elements of W. The first 16 PSF components sorted by their relative weights are shown in Fig. 1. The indexes show the order while the PSF component with $N = 0$ representing the largest one. It is obvious that the PSF components with higher indexes are disturbed by noises significantly, no effective profile or distribution can be found. The relative weights of these PSF components are very low, as shown in Fig. 2, the cumulative weight of the first 5 components can reach up to nearly 70%.

For PCA components with relatively small weights, it is considered that the related PSF patterns are not important, or most of them only exhibit noise structures. Generally the noise structures in the PSF components arise from the

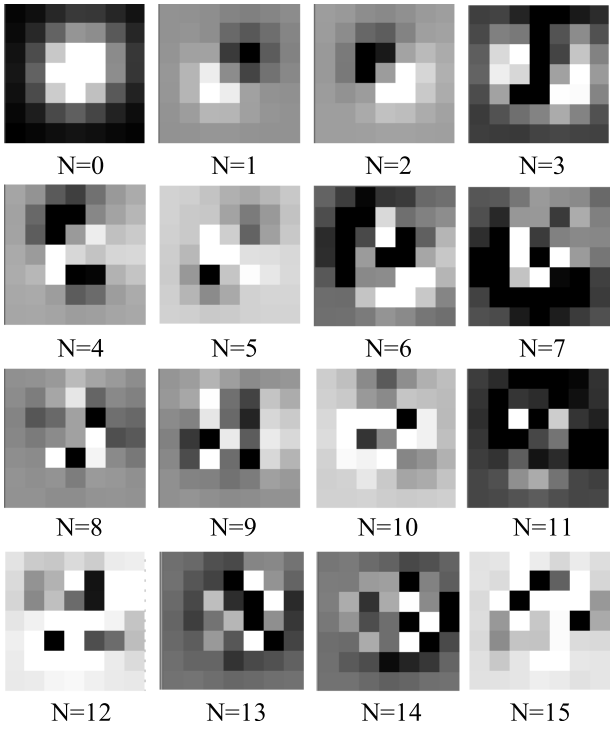

Figure 1. The first 16 *PSF components decomposed from our test data set.*

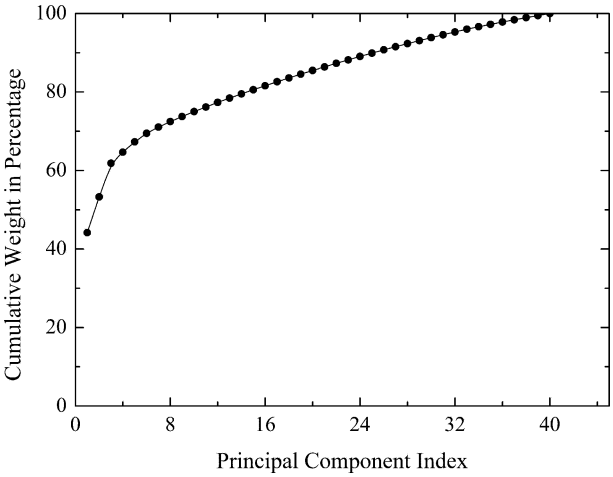

Figure 2. The cumulative weight of the first 40 *PSF components.*

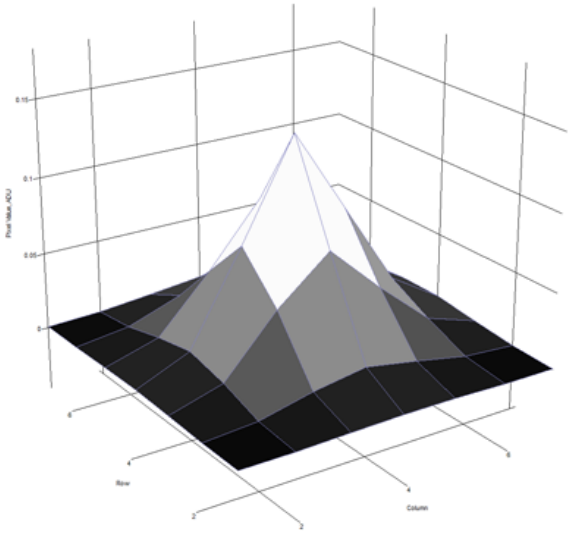

Figure 3. The surface plot of the PSF model constructed with PCA.

optics defects and are randomly distributed, while the effective PSF components are statistically efficient and optimal for all PSF samples, the relative weights of the effective components drop dramatically in high order components. Hence after arranging the PSF components according to their weights, the effective ones are selected and generated to the final PSF model adopted in restoration. As shown in Fig. 3.

3. APPLICATION

To test the efficiency of our technique and the promotion in source detection, another trial observation is performed for surveying space debris. The trial observation lasted for 11 nights between 17th December 2017 and 8th January 2018. According to the dynamical features of high Earth orbital objects[12], stare mode is the best choice for the exposure, which makes the candidate images shown as points and maximize their SNR. Hence in our survey stare mode is adopted, the telescope turns to the scheduled horizontal pointing, consecutive CCD raw frames are acquired with the same azimuth and elevation. For each night about 240 fields were surveyed, the field was switched every minute and it leaded to a 4 hours survey in total. Considering the apparent brightness of space debris is generally high, for most cataloged objects the apparent magnitude is less than 16, the single exposure was 2 seconds and for each field around 15 raw CCD frames can be acquired, taking into account the time interval due to CCD frame readout and the pointing setting of telescope.

The detail schedule of the survey fields in the horizontal system is shown in Fig. 4, the survey azimuth is arranged from 136° to 207°, and the elevation is arranged from 51° to 65°. For each night, the survey was repeated with the same ordered schedule. It should be noticed that due

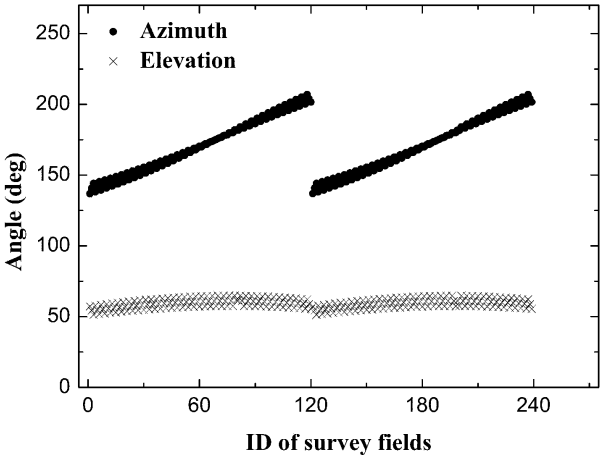

Figure 4. The schedule of the survey fields in horizontal coordinates.

to the survey schedule one object may be observed several times in one night, and it is common in space debris observations, multiple arcs in short time interval help to determine the orbit and trajectory more precisely.

Based upon the data, our dedicated pipeline is adopted to extract the arcs which consist of a series of measurement positions of the same object through consecutive frames and estimate their equatorial positions, then the arcs are correlated with the catalog, the number of detected objects and false detections will be obtained. It should be noticed that the same parameters and options are adopted in our pipeline while reducing both the raw data and the restored data, and with the comparison of the results for the raw data and the restored data, the improvement of our technique will be investigated.

4. RESULTS AND DISCUSSIONS

The preliminary results of the raw data is listed in Table. 2. With the wide field of view telescope, in average more than 500 arcs can be extracted each night in the survey, which are correlated to more than 60 space objects from the catalog. The false detection rate is less than 2.5% in average and the correlation ratio is stable through the whole survey, hence the validation of our observing strategy and the reduction pipeline is proved. While the results of the restored data is shown in Table. 3, it is demonstrated that the detected arcs and the objects correlated are increased distinctly, although the improvement is not stable through the surveys. It may be caused by the unexpected impulse noises which are mainly generated due to the cooling errors of the CCD camera, and the count of objects located in the survey field also affects the improvement, which means if all objects are observed with high SNR they will be extracted all from raw images, the restoration exhibits no improvement. The improvement of our technique is shown in Table. 4. It can be easily found that the correlation ratio is decreased for the restored data, due to the fact that additional noises are

Table 2. Statistics of the measurement information for raw images.

Date (UTC)	Arcs detected	Arcs correlated	Ratio (%)	Objects
20171217	353	340	96.3	60
20171219	276	266	96.4	50
20171222	378	374	98.9	65
20171223	385	372	96.6	64
20171224	271	258	95.2	54
20171225	402	388	96.5	60
20171228	292	282	96.6	60
20171229	268	258	96.3	60
20180105	439	439	100.0	68
20180106	437	437	100.0	71
20180108	401	392	97.8	64

Table 3. Statistics of the measurement information for restored images.

Date (UTC)	Arcs detected	Arcs correlated	Ratio (%)	Objects
20171217	580	526	90.7	75
20171219	1038	519	50.0	90
20171222	652	548	84.0	82
20171223	681	548	80.5	82
20171224	664	432	65.1	84
20171225	657	546	83.1	74
20171228	370	360	97.3	60
20171229	302	292	96.7	60
20180105	673	601	89.3	82
20180106	707	627	88.7	87
20180108	697	547	78.5	81

recognized as objects, however, it is acceptable for the tradeoff between the increased detected object count and the false detections introduced.

5. CONCLUSIONS

In our paper, a technique for improving the detection ability for space debris utilizing wide field of view and relatively small aperture telescope is presented. In detail, the image restoration is adopted to improve the image quality and detection efficiency, and for optimization of image processing, the PSF is modeled from large amounts of raw CCD images with principal component analysis, the preliminary results are analyzed and the optimal mean point spread function is constructed, with which the image restoration is performed to improve the data quality and reduction efficiency. A trial survey is performed with our wide field of view ($4.4^\circ \times 4.4^\circ$) 50-cm refracting telescope, and a dedicated image processing pipeline for detecting GEO objects automatically is adopted. Our survey lasts for 11days and it takes 4 hours each day. After the raw images are obtained, the restoration is performed with our proposed technique, then the image processing pipeline runs on both raw and restored images. The tracklets are correlated with the catalog and the improvement

Table 4. Improvement of the restoration.

Date (UTC)	Arcs increase	Increase ratio (%)	Objects increase	Increase ratio (%)
20171217	227	64.3	15	25.0
20171219	762	276.1	40	80.0
20171222	274	72.5	17	26.1
20171223	296	76.9	18	28.1
20171224	393	145.0	30	55.6
20171225	255	63.4	14	23.3
20171228	78	26.7	0	0
20171229	34	12.7	0	0
20180105	234	53.3	14	20.6
20180106	270	61.8	16	22.5
20180108	296	73.8	17	26.6

for object detection is investigated accordingly. The results demonstrates that with image restoration, the count of tracklets increases about 80% in average, and the count of objects detected increases more than 20% for most atcs. Due to the smear noises and unexpected impulse noises, the correlation ratio of the tracklets varies and is reduced by around 10% for most surveys. The efficiency of our techniques is proved, and it should be noted that with imaging modeling and restoration, the detection ability can be improved distinctly with the present technical state of art.

ACKNOWLEDGMENTS

Our work was funded by the National Natural Science Foundation of China (Grant Nos. 11533010, 11703096 and U1631133), and the Natural Science Foundation of Jiangsu Province (Grant No. BK20171110)

REFERENCES

1. Ping Y. D., Zhang C., (2017), Advances in Space Research, 60, 907
2. Jia P., Sun R. Y., Wang W. N., et al., (2017), Monthly Notices of the Royal Astronomical Society, 470, 1950
3. Wang W. N., Jia P., Cai D. M., et al., (2018), Monthly Notices of the Royal Astronomical Society, 478, 5671
4. Sun R. Y., Zhao C. Y., (2014), Research in Astronomy and Astrophysics, 14, 992
5. Sun R. Y., Zhao C. Y., (2013), Research in Astronomy and Astrophysics, 13, 604
6. Sun R. Y. et al., (2015), Acta Astronautica, 110, 9
7. Nunez J., Nunez A., Montojo F. J., et al., (2015), Advances in Space Research, 55, 218
8. Starck J. L., Murtagh F., (2006), Astronomical Image and Data Analysis (Berlin, Springer)
9. Jee M. J., Blakeslee J. P., Sirianni M., et al., (2007), Publications of the Astronomical Society of the Pacific, 119, 1403

10. Jee M. J., Tyson J. A., (2011), Publications of the Astronomical Society of the Pacific, 123, 596

11. Sun R. Y., Jia P., (2017), Publications of the Astronomical Society of the Pacific, 129, 044502

12. Zhao C. Y., Zhang M. J., Wang H. B., et al., (2013), Advances in Space Research, 52, 677